

# ***Design and Fabrication of A High-Performance Polysilicon Vibrating Ring Gyroscope***

Farrokh Ayazi, and Khalil Najafi  
*Center for Integrated Sensors and Circuits*  
University of Michigan, Ann Arbor, MI 48109-2122, USA  
e-mail: ayazi@engin.umich.edu, Tel: (313) 936-2954, Fax: (313) 647-1781

## **ABSTRACT**

This paper presents a detailed analysis on the design and scaling limits of vibrating ring gyroscopes and their implementation using a combined bulk and surface micromachining technology. A high aspect-ratio p++/polysilicon trench-refill fabrication technology has been used to realize the 30-40 $\mu$ m thick polysilicon ring structure with 0.9 $\mu$ m ring-to-electrode gap-spacing. The theoretical analysis of the ring gyroscope shows that by taking advantage of the high quality factor of polysilicon, sub-micron ring-to-electrode gap spacing, high aspect ratio polysilicon ring structure produced using deep dry-etching, and the all-silicon feature of this technology, tactical grade vibrating ring gyroscopes with random walk as small as 0.05 deg/ $\sqrt{h}$  can be realized, providing several orders of magnitude improvement in performance.

**Keywords:** Gyroscope, yaw rate sensor, high aspect ratio polysilicon

## **INTRODUCTION**

Micromachined silicon gyroscopes have received a lot of attention during the past few years. Much of the effort has concentrated on developing "rate grade" devices for automotive applications which require a rotation rate resolution and bias stability of about 0.1 deg/sec. Nickel-plated vibrating rings [1,2] and surface micromachined polysilicon tuning forks [3,4] are examples of these "rate grade" gyroscopes. There are, however, several applications which require improved performance, including inertial navigation, guidance, and some consumer electronics. Achieving "tactical and inertial grade" performance levels, i.e., resolution and bias stability better than 1-10 deg/h and high scale factor accuracy, has proven to be a tough challenge, and new technologies and approaches have to be developed to allow micromachined gyroscopes achieve this level of performance. Draper Lab's silicon tuning fork gyroscope [5], JPL/UCLA clover-leaf [6] and Bosch yaw rate sensor [7] are the latest precision micromachined gyroscopes that have been so far reported in the literature. These either have complicated fabrication processes or suffer from not having very stable and symmetric structures. In addition, in some of these approaches, the output signal from the device is rather small, which limits its overall sensitivity.

This paper presents results obtained from the first phase in the development of next-generation micromachined gyroscopes aimed at a performance improvement of several orders of magnitude. To accomplish this, several steps have been undertaken. First, a vibrating ring gyroscope [1] has been selected as the sensor structure. Second, a detailed analysis has been performed to determine its overall sensitivity and identify its scaling limits. Several aspects of this analysis apply to other gyroscope sensing structures and are discussed in detail. Based on this analysis, a single-wafer, all-silicon, high aspect-ratio p++/polysilicon trench-refill technology has been developed to implement sensor structures that provide features required for achieving the desired high performance. The following sections will discuss the above three areas in detail. The paper concludes with the presentation of preliminary experimental results showing fabricated structures.

## **VIBRATING RING GYROSCOPE**

The vibrating ring gyroscope consists of a ring, semi-circular support springs, and drive, sense and control electrodes (Fig. 1) [1]. The ring is electrostatically vibrated into an elliptically-shaped primary flexural mode with a fixed amplitude. When device is subjected to rotation, Coriolis force causes energy to be transferred from the primary mode to the secondary flexural mode, which is located 45° apart from the primary mode, causing amplitude to build up proportionally in the latter mode; this build-up is capacitively monitored.

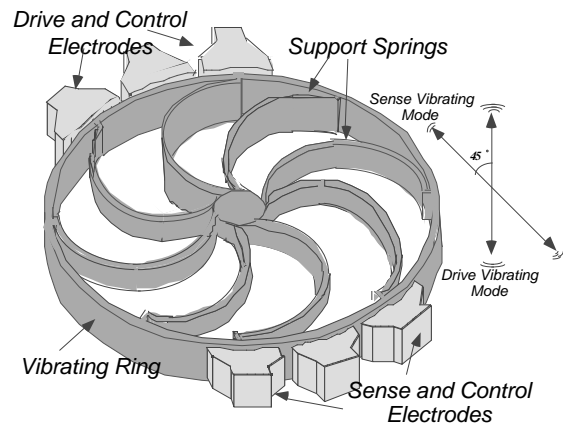


**Figure 1:** Structure of a Vibrating Ring Gyroscope[1].

Among the different types of vibratory gyroscopes, the vibrating ring structure has some unique features: •the inherent symmetry of the structure makes it less sensitive to spurious vibrations; •since two identical flexural modes of the structure with nominally equal resonant frequencies are used to sense rotation, the sensitivity of the sensor is amplified by the quality factor of the structure, resulting in higher sensitivity; and, •the vibrating ring is less temperature sensitive since the vibration modes are affected equally by temperature.

A nickel-plated micromachined vibrating ring gyroscope had been previously reported [1,2], and demonstrated a resolution of  $\sim 0.5$  deg/sec in a 10 Hz bandwidth. The nickel electroforming technology used for this device poses several drawbacks to improved device performance, including: 1) a fairly large ring to electrode gap spacing were achievable in the conventional electroplating process, which resulted in a small sense capacitance; although this could be overcome by more sophisticated technologies like LIGA, it is not desirable to use these because of cost considerations; 2) the thermal expansion coefficient of the silicon substrate is different than the sensor element, which was made out of nickel. Therefore as the temperature changes, the ring expands (or shrinks) more than the electrodes, which are attached to the substrate, causing the ring-to-electrode gap spacing to change; this in turn results in an increased temperature sensitivity of offset and scale factor; and 3) worse material properties resulting in much lower Q, and higher potential for creep, fatigue and long-term drift.

To overcome these shortcomings, we have developed a new all-silicon vibrating ring gyroscope structure, as illustrated in Figure 2, fabricated using a p++/polysilicon trench-refill technology [8]. The vibrating ring and support springs are created by refilling deep dry-etched trenches with polysilicon deposited over a sacrificial LPCVD oxide layer, as shown in Fig. 2. Each sense electrode is made from a p++ silicon island (12 $\mu$ m deep) hanging over an EDP-etched pit. The p++ islands are all anchored on top to a supporting polysilicon layer, which is anchored through an isolating nitride layer to the substrate. The polysilicon ring is anchored in the middle to the substrate and is suspended over the etch pit using support springs. This structure allows the polysilicon ring to be made as thick as the deep RIE step used for forming the trench allows, permits the formation of extremely narrow air gaps through sacrificial layer etching, and utilizes polysilicon with its superior and homogenous material properties. In addition, because of the high aspect ratio and the large device thickness, the ring radius can be easily increased, thus reducing the resonant frequency and increasing the sense capacitance.

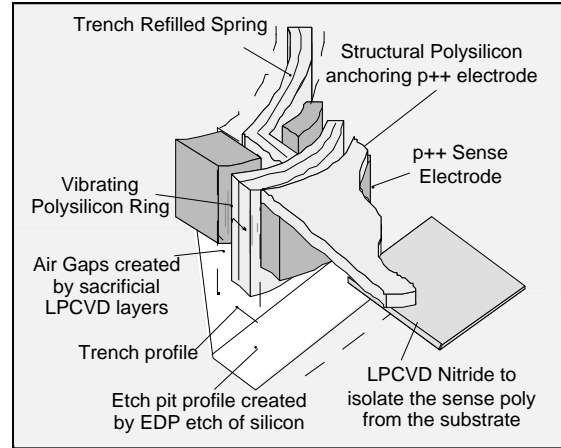


**Figure 2:** The new vibrating ring gyroscope utilizing polysilicon to form the thick, high aspect ratio ring, and p++ microstructures for sense/drive electrodes.

These features play an instrumental role in allowing the performance of the vibrating ring gyroscopes to be improved by orders of magnitude as indicated in the detailed analysis presented below.

### SENSITIVITY ANALYSIS

Vibration of the ring gyroscope causes the electrode gap to vary as a function of time and position along the electrode. In order to vibrate the ring in an elliptically shaped mode that has two nodal diameters (flexural mode), a sinusoidal electrostatic drive force is applied through the surrounding electrode located at a reference zero degree point. Figure 3 shows the detection scheme used to sense ring vibrations [1]. The ring is set at a polarization voltage  $V_p$  to provide the bias for capacitive detection. The drive electrode (located at  $0^\circ$ ) is driven by an ac drive voltage ( $v_d$ ) which combines with the polarization voltage  $V_p$ . The ac voltage developed at the sense electrode (located at  $45^\circ$ ),  $v_s$ , is generated by the vibration of the ring which is biased at  $V_p$ . A simple source follower is assumed to be used as the buffer amplifier to sense the ring vibrations. The input bias voltage of the amplifier,  $V_{bias}$ , is set through an isolated minimum geometry diode.

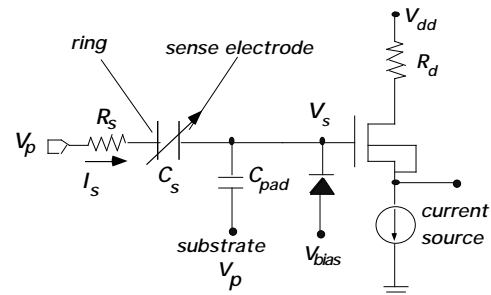


**Figure 3:** Detection scheme used to sense ring vibration.

For the sense electrode,  $V_s = V_{bias} + v_s$ , where  $V_{bias}$  is the bias voltage applied through the input diode and  $v_s$  is the ac sense voltage.  $I_s$ , the current flowing through the combination of the sense electrode capacitance ( $C_s$ ) and the capacitance associated with the output pad to the substrate ( $C_{pad}$ ) (substrate is assumed to be at the polarization voltage  $V_p$ ) is injected into the gate of the source follower and can be expressed by:

$$I_s = \frac{d}{dt}(Q) = \frac{d}{dt} \left[ (C_d + c_d + C_{pad})(V_p - V_{bias} - v_s) \right] \quad (1)$$

where  $C_d$  and  $c_d$  are the average and the time varying components of the ring to sense electrode capacitance ( $C_s$ ), respectively.  $R_s$  is the series resistance associated with the path connecting the point where  $V_p$  is applied to the ring itself; due to the high doping level of polysilicon, this resistance is negligible compared to the impedance of the sense capacitance, and for simplifying purposes it is assumed to be zero. If the input capacitance of the buffer amplifier is  $C_{inp}$ , one can find an expression for  $v_s$  as:

$$v_s = \frac{c_d}{(C_d + C_{pad} + C_{inp})} (V_p - V_{bias}) \quad (2)$$

Expression (2) states that in order to get higher sensitivity, the amount of change in ring to sense electrode capacitance due to the ring vibration should be maximized while the total sum of  $C_d + C_{pad} + C_{inp}$  should be minimized. So, a buffer amplifier with very small input capacitance must be used and the output pad capacitance to the substrate should be minimized. The electrode capacitance can be expressed by:

$$C_s = \frac{h}{d_0 + d} \cdot r \cdot d \quad (3)$$

where  $d_0$  is the equilibrium gap spacing,  $d$  is the change in the gap due to vibration,  $h$  is the height of the structure,  $r$  is the radius of the ring and  $\theta$  is the angle faced by each electrode. As mentioned earlier, the ring vibrates in elliptically shaped mode patterns that have two node lines. In polar coordinates,  $d = (q_1 r_1 + q_2 r_2)$ , where the radial mode shape functions  $r_1$  and  $r_2$ , for the ring portion of the sensor structure alone, are given by the expressions:

$$r_1 = \cos(2\theta - 2\theta_0) \quad \text{and} \quad r_2 = \sin(2\theta - 2\theta_0) \quad (4)$$

$\theta_0$  is the location of the antinode of the normal mode. In order to simplify the math, we can assume that  $\theta_0$  is equal to zero; also for the sense electrode located at the  $45^\circ$  position,  $r_2$  would be much larger than  $r_1$ , allowing us to assume that  $d \approx q_2 r_2$  ( $q_2$  is the amplitude of the

secondary vibration mode of the ring). Therefore, we can simplify equation (3) by neglecting the higher order terms to:  $C_s \approx C_d + c_d$ , where:

$$C_d = \frac{h \cdot r}{d_0} \quad \text{and} \quad c_d = \frac{h \cdot r}{d_0^2} \cdot \sin(\theta) \cdot q_2 \quad (5)$$

Now, if we combine equation (2) and equation (5), the following expression for the amplitude of the sense voltage developed at the  $45^\circ$  electrode can be obtained:

$$v_s = \frac{(V_p - V_{bias})}{(C_d + C_{pad} + C_{inp})} \cdot \frac{h \cdot r \cdot \sin(\theta)}{d_0^2} \cdot q_2 \quad (6)$$

In this equation,  $q_2$  is determined by  $q_1$ , the amplitude of the primary mode and the rotation sensitivity of the structure. The rotation sensitivity of the shell structure is given by [9]:

$$\frac{q_2}{q_1} = 4A_g \cdot Q \cdot \omega \quad (7)$$

where  $A_g$  is the angular gain (depends on the geometry of the sensor and is 0.37 for the ring structure),  $Q$  is the quality factor,  $\omega$  is the angular resonant frequency and  $\dot{\theta}$  is the rotation rate. The vibration amplitude of the ring,  $q_1$ , should be set as large as possible to increase the sensitivity but, it must be kept typically below 5% to 10% of the equilibrium gap spacing,  $d_0$ , to avoid the nonlinear effects of the electrostatic force. Therefore,  $q_1 = k \cdot d_0$ , where  $k \approx 0.1$ ; The minimum detectable rotation rate for the vibrating shell structure,  $\omega_{s(min)}$ , is directly proportional to the minimum detectable sense voltage,  $v_{s(min)}$ , which will be determined by the input equivalent noise of the output buffer amplifier. If we assume that the buffer noise,  $V_n$ , has a white spectrum and the detection circuit has a bandwidth  $BW$ , then the minimum detectable rotation rate is given by:

$$\omega_{s(min)} = \frac{(C_d + C_{pad} + C_{inp})}{4kA_g (V_p - V_{bias})} \cdot \frac{d_0 \sqrt{BW}}{h \cdot r \cdot \sin(\theta)} \cdot \frac{1}{Q} \cdot V_n \quad (8)$$

This equation shows that the sensitivity of the ring gyroscope can be improved by: •increasing the quality factor ( $Q$ ); •reducing the ring-to-sense electrode gap spacing ( $d_0$ ); •lowering the resonant frequency ( $\omega$ ); •increasing the height of the sense electrodes ( $h$ ) and radius of the ring ( $r$ ) as well as the angle faced by each sense electrode ( $\theta$ ); •decreasing the total parasitic and rest capacitances ( $C_d + C_{pad} + C_{inp}$ ); •minimizing circuit input noise; and finally •increasing  $V_p$ .

The Brownian noise of the structure which is the fundamental limiting noise component of the mechanical structure only, is given by the following expression:

$$z_{(Brownian)} = \frac{1}{2A_g q_1} \sqrt{\frac{k_B T}{MQ^3}} \quad (9)$$

where  $M$  is the generalized mass of the vibration mode. For the polysilicon ring gyroscope, this will correspond to a  $z_{(Brownian)}$  less than  $1 \times 10^{-6} \text{ deg/sec}/(\text{Hz})^{0.5}$ .

### Resonant Frequency

The natural frequency for the radial-circumferential flexural modes of a cylindrical shell with a radius  $r$  and a shell thickness  $t$  is given by [10]:

$$f_i = \frac{1}{2} \frac{1}{\sqrt{12}} \frac{t}{r^2} \frac{i(i^2 - 1)}{\sqrt{(i^2 + 1)}} \sqrt{\frac{E}{\rho}} \quad i = 2, 3, 4, \dots \quad (10)$$

where  $E$  is the Young's modulus and  $\rho$  is the density of the shell material. Natural frequencies of the flexural modes are independent of the height of the shell structure. Using equation (10), it is possible to calculate the flexural resonant frequency of the ring gyroscope. Since the radius of each supporting spoke is approximately equal to half of the radius of the ring itself, stiffness of each spoke can be calculated to be 4 times larger than the stiffness of the ring shell without any spoke attached to it. Therefore, the overall stiffness for the flexural mode of the ring gyroscope will be 5 times the stiffness of the shell structure and the natural frequency for the first flexural mode of the ring can be stated as ( $i=2$  in equation (10)):

$$f_{ringgyro} = \frac{1}{2} \frac{6}{\sqrt{12}} \frac{t}{r^2} \sqrt{\frac{E}{\rho}} \quad (11)$$

In case of the polysilicon ring gyroscope, if we assume that the Young's modulus of polysilicon is approximately equal to  $E=150 \text{ GPa} = 1.5 \times 10^{12} \text{ dynes/cm}^2$  and its density is equal to  $\rho_{si}=2.328 \text{ g/cm}^3$ , for a cylindrical ring with a radius of  $500 \mu\text{m}$  and a shell thickness of  $3.6 \mu\text{m}$ , the resonant frequency of the first flexural mode can be calculated to be equal to  $f_{ringgyro} = 33 \text{ kHz}$ .

In order to find the range of polarization voltages  $V_p$  that can be applied to the ring structure, we need to calculate the pull-in voltage between the ring and each sense electrode. Using the parallel plate approximation, the pull-in voltage can be expressed as:

$$V_{Pull-in} = \frac{2}{3} \frac{K_z}{A} d_0^{1.5} \quad (12)$$

The flexural stiffness of the ring structure can be calculated using the following expression:

$$K_z = 12 E h \frac{t^3}{r} \quad (13)$$

In calculating the sense area ( $A$  in eqn. 12), the effective height for each sense electrode is determined by the height of deep boron diffusion which is approximately equal to  $12 \mu\text{m}$ . However, by increasing the height of the ring ( $h$  in eqn. 13), one can make the structure stiffer and increase the pull-in, and hence the polarization, voltage. For prototype devices with  $h=35 \mu\text{m}$  and gap spacing  $d = 1 \mu\text{m}$ , the pull-in voltage is calculated to be  $V_{pull-in}=32 \text{ Volts}$ .

Table 1 compares the design parameters and performance of the first generation nickel and the second generation polysilicon ring gyroscopes. For polysilicon ring gyro,  $C_d = 15 \text{ fF}$ ;  $C_{pad} = 160 \text{ fF}$ ;  $C_{inp} = 50 \text{ fF}$ . Assuming that  $(V_p - V_{bias}) = 25 \text{ Volts}$ , for a circuit noise level of  $V_n = 1 \mu\text{V}/(\text{Hz})^{0.5}$ , the minimum detectable rotation rate of the Polysilicon Ring Gyroscope can be approximately calculated to be  $0.8 \times 10^{-3} \text{ deg/sec}/(\text{Hz})^{0.5}$  ( $0.05 \text{ deg}/\sqrt{h}$ ) which is equivalent to a resolution of  $2.5 \times 10^{-3} \text{ deg/sec}$  in a  $10 \text{ Hz}$  bandwidth, a factor of 200 improvement compared to the Nickel gyroscope.

**Table 1.** Specifications and calculated performance of the Polysilicon Gyroscope and comparison with Ni Gyroscope.

Design Parameter	Nickel Gyroscope	Poly-Si Gyroscope
Material Quality Factor	2000	>40,000
Ring Diameter	1 mm	1 mm
Ring-Electrode Gap Spacing	7 $\mu\text{m}$	1.0 $\mu\text{m}$
Ring and Springs Width	6 $\mu\text{m}$	3 $\mu\text{m}$
Height of Ring Structure	19 $\mu\text{m}$	35 $\mu\text{m}$
Number of Electrodes	32	16
Height of Each Electrode	19 $\mu\text{m}$	12 $\mu\text{m}$
Calculated Resonant Freq.	30 kHz	33 kHz
Min. Detectable Signal (10Hz BW)	0.5 deg/sec	$2.5 \times 10^{-3} \text{ deg/sec}$

### FABRICATION TECHNOLOGY

A high aspect ratio p++/polysilicon trench-refill technology [8] has been used to fabricate the Polysilicon Ring Gyroscope (PRG). The fabrication process requires seven masks and the sequence is shown in Figure 4. The vibrating ring and the support springs are created by refilling deep dry-etched trenches with polysilicon deposited over a sacrificial LPCVD oxide layer. The depth of the trench primarily determined by the etching system used for its formation and can now be made to be as deep as several hundred microns. The ring-to-electrode gap spacing is defined by the thickness of the sacrificial oxide layer and therefore, it can be reduced to sub-micron levels, increasing the sense capacitance and hence

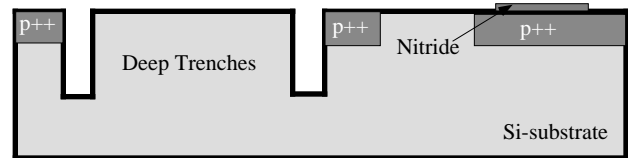
improving the resolution of the device. The structural polysilicon layer is doped with phosphorous to lower its electrical resistance. Each sense electrode is made from a p++ silicon island (12 $\mu\text{m}$  deep boron diffusion). The p++ islands are all anchored on top to the supporting polysilicon layer, which is anchored through an isolating nitride layer to the substrate. This LPCVD nitride layer is 2000 $\text{\AA}$  thick and acts as the isolation dielectric layer underneath the electrode bonding pad. Polysilicon vertical stiffeners (trench-refilled) are also incorporated to ensure the rigidity of each sense electrode structure. A protective LPCVD oxide layer will completely encapsulate the poly to protect it during the EDP etch. This oxide is then patterned to form metal contacts and openings to the silicon substrate for the subsequent EDP release step. After patterning the oxide, Cr/Au (300 $\text{\AA}$ /4000 $\text{\AA}$ ) is sputtered and lifted-off to form electrode bonding pads. The sense electrodes and the ring are then released and separated from one another using an EDP etch (108 $^{\circ}\text{C}$  for 2.5 hours), which dissolves the undoped part of the substrate, followed by the etching of the sacrificial oxide in HF:H<sub>2</sub>O solution to completely release the structure.

### FABRICATION RESULTS

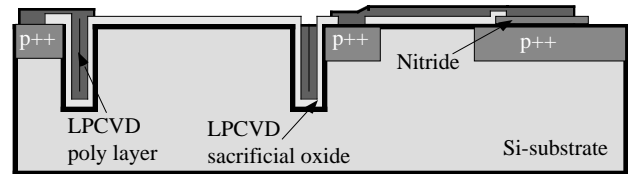
Prototypes of the Polysilicon Ring Gyroscope have been successfully fabricated. Figure 5 shows an SEM picture of a 1.7mm $\times$ 1.7mm Polysilicon Ring Gyroscope. The polysilicon ring is 1mm in diameter, 3.5 $\mu\text{m}$  wide and 35 $\mu\text{m}$  tall. Sixteen electrodes are evenly located around the ring structure; the support post is 100 $\mu\text{m}$  in diameter.

Figure 6 shows a close-up view of one of the sense electrodes, showing how each p++ sense electrode is anchored through the polysilicon layer to the substrate. The 0.9 $\mu\text{m}$  ring-to-electrode gap spacing is more clearly shown in Figure 7; the high aspect ratio polysilicon ring, spring, and the p++ sense electrode are all suspended over the EDP-etched pit. In this figure, the high aspect-ratio 3.5 $\mu\text{m}$  wide, 35 $\mu\text{m}$  tall polysilicon ring with smooth vertical sidewalls is also clearly visible. The ring is made by refilling 5.5 $\mu\text{m}$  wide, 36 $\mu\text{m}$  deep, dry-etched trenches right after deposition of a 1 $\mu\text{m}$  sacrificial oxide layer.

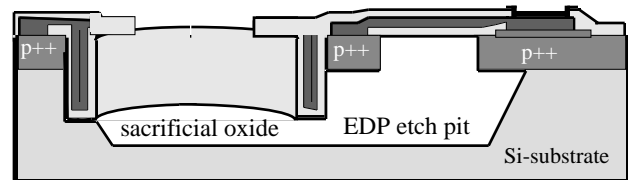
The Polysilicon Ring Gyroscope provides several important features required for high-performance devices. First, since the ring-to-electrode gap spacing is defined by the thickness of the sacrificial layer, it can be made <1 $\mu\text{m}$ , thus increasing the sense capacitance. Second, the height of the structure can be arbitrarily increased, which in turn allows the ring radius to be increased without making the structure too compliant, thus reducing the resonant frequency and increasing the sense capacitance. Third, the structural material is polysilicon which has a high Q, and an orientation independent Young's modulus.



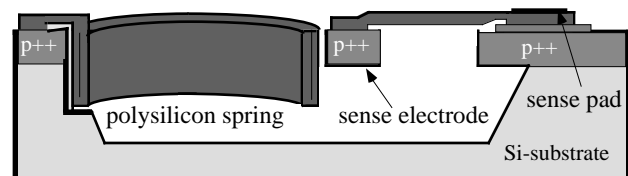
a) Deep boron diffusion (p++) to define the electrodes and support post; b) Deposit and pattern the isolating nitride layer; c) Dry etch deep trenches to define the ring structure.



d) Deposit and pattern the LPCVD sacrificial oxide layer; e) Refill trenches with structural LPCVD polysilicon layer (n-doped); f) Pattern the polysilicon layer.



g) Deposit and pattern the encapsulating oxide layer; h) Deposit and pattern Cr/Au; i) EDP etch to release and separate electrodes;



i) Etch the sacrificial oxide layer and completely release the structure.

**Figure 4:** Fabrication process for polysilicon ring gyro.

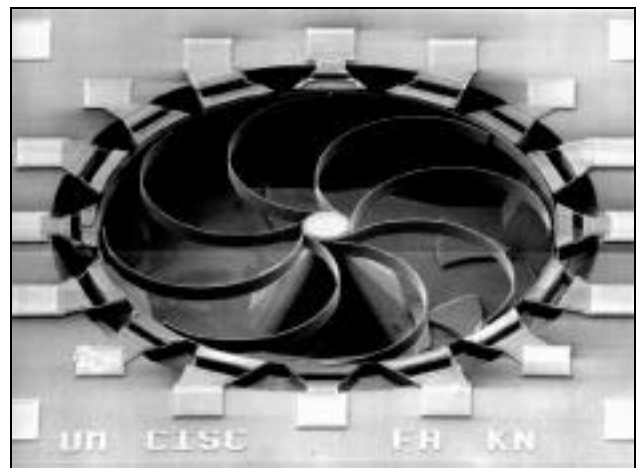


**Figure 5:** SEM view of a Polysilicon Ring Gyroscope. The ring is 1mm in diameter, 3  $\mu\text{m}$  wide and 35  $\mu\text{m}$  tall.

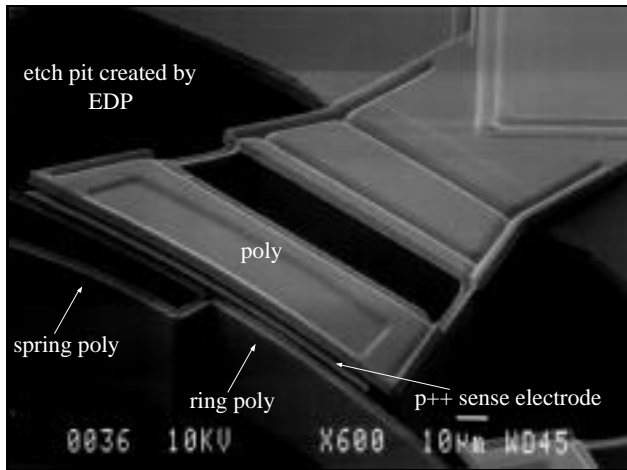


**Figure 6:** Close-up of a suspended p++ sense electrode anchored on top to the supporting polysilicon layer.

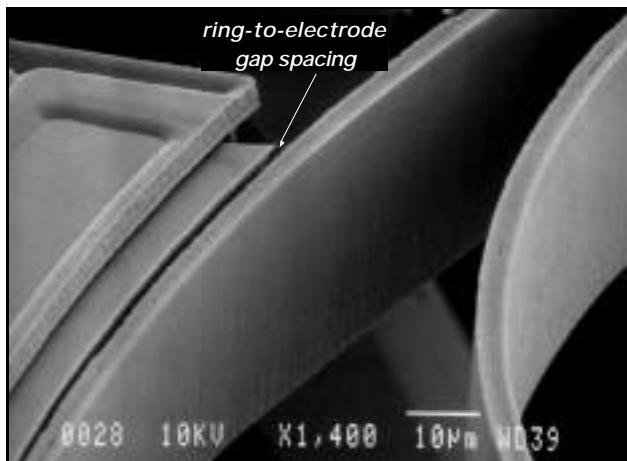


**Figure 7:** SEM view of the 0.9µm ring-electrode gap.

Only preliminary tests have been performed on the realized structures. Figure 8 shows the measured resonance behavior of the first flexural mode of a polysilicon ring. The resonant frequency is ~36kHz which agrees with calculated values. This experiment was carried out with a  $(V_p - V_{bias}) = 1$  Volt under low vacuum levels. More detailed measurements and characterization will have to be performed in the future, which is the next phase of our program aimed at development of high-performance micromachined gyroscopes.

### CONCLUSIONS

Design and fabrication of the first polysilicon vibrating ring gyroscope using a single-wafer high aspect ratio p++/polysilicon trench-refill technology have been reported. It is shown through analysis that sub-micron ring-to-electrode gap spacing, high-aspect-ratio ring structure and high quality factor of polysilicon as the structural material can improve the performance of the polysilicon ring gyroscope by orders of magnitude. This

will be experimentally verified using the structures fabricated and reported in this paper.

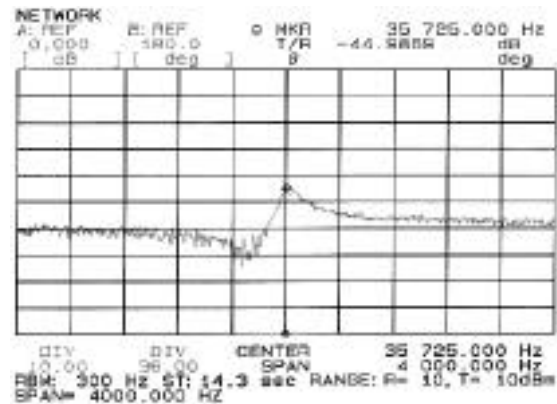


**Figure 8:** The first flexural resonant peak of a prototype Polysilicon Ring Gyroscope.

### ACKNOWLEDGMENTS

The authors would like to acknowledge Dr. Mike W. Putty (of General Motors research Center), and Dr. Arjun Selvakumar for their contributions. This work was supported by the DARPA/ETO MEMS program under contract # DABT63-C-0111.

### REFERENCES

- [1] M. W. Putty, K. Najafi, "A Micromachined Vibrating Ring Gyroscope", *Digest, Solid-State Sensors & Actuators Workshop*, Hilton Head, SC, p. 213, 1994
- [2] D. R. Sparks et al, "A CMOS Integrated Surface Micromachined Angular Rate Sensor: Its Automotive Applications", *Digest, Transducers '97*, Chicago, p. 851
- [3] W. A. Clark and Roger T. Howe, "Surface Micromachined Z-Axis Vibratory Rate Gyroscope", *Digest, Solid-State Sensors and Actuators Workshop*, Hilton Head, SC 1996, p. 283
- [4] K. Y. Park et al, "Laterally Oscillated and Force-balanced Micro Vibratory Rate Gyroscope Supported by Fish Hook Shape Springs", *Digest, IEEE/ASME Micro Electro Mechanical Systems Workshop*, 1997, p. 494
- [5] M. Weinberg et al, "Micromachining Inertial Instruments", *SPIE's Symposium on Micromachining & Microfabrication*, Austin, TX, 1996
- [6] T. K. Tang et al, "Silicon Bulk Micromachined Vibratory Gyroscope", *Digest, Solid-State Sensors and Actuators Workshop*, Hilton Head, SC, p. 288, 1996
- [7] M. Lutz et al, "A Precision Yaw Rate Sensor in Silicon Micromachining", *Digest, Transducers '97*, Chicago, June 1997, p. 847
- [8] A. Selvakumar, K. Najafi, "High Density Vertical Comb Array Microactuators Fabricated Using a Novel Bulk/Poly-Silicon Trench Refill Technology", *Digest, Solid-State Sensors and Actuators Workshop*, Hilton Head, SC, June 1994, p. 138.
- [9] M. W. Putty, "A Micromachined Vibrating Ring Gyroscope", Ph.D. Thesis, Univ. Michigan, March 95.
- [10] H. A. Rothbart, "Mechanical Design Handbook", McGraw-Hill, 1996.